Electron Spin Resonance Study of Electron Transfer Rates in DNA: Determination of the Tunneling Constant β for Single-Step Excess Electron Transfer

Andrea Messer, Kristopher Carpenter, Kristen Forzley, John Buchanan, Shen Yang, Yurii Razskazovskii,† Zhongli Cai, and Michael D. Sevilla*

Department of Chemistry, Oakland University, Rochester, Michigan 48309

Received: October 5, 1999; In Final Form: December 2, 1999

An investigation of electron transfer in DNA at low temperatures in an aqueous glassy medium is reported for a system in which electrons are generated by radiation and trapped on DNA. The transfer of the electron from the DNA anion radical to randomly interspaced intercalators is followed by electron spin resonance spectroscopic observation of the buildup in the intercalator electron adduct electron spin resonance (ESR) signal and the loss of the DNA anion signal with time at 77 K. The intercalators investigated, mitoxantrone, ethidium bromide, 1,10-phenanthroline, and 5-nitro-1,10-phenanthroline, test the effect of charge and electron affinity. The time frame of the experiment, minutes to weeks, allowed the use of large intercalator spacings (low loadings) at which random intercalation is most likely. The fraction of the electron captured by the intercalator was found to increase with ln(t) as expected for a single-step tunneling process. Fits of results to expressions for electron capture by intercalators based on a random distribution suggest that the random model is appropriate up to loadings of about 1 per 10−20 DNA base pairs depending on the intercalator. The distances of electron-transfer range from 4 base pairs (ethidium) to 10 base pairs (mitoxantrone) after 1 min at 77 K. The low temperatures employed allow for the observation of single-step tunneling free from competing mechanisms such as hopping. The values of the tunneling constant β found, 0.8−1.2 Å^{-1}, do not suggest that tunneling through the DNA base stack provides a particularly facile route for transfer of *excess* electrons through DNA. We find that the transfer distances and rates correlate with intercalator electron affinities calculated by density functional theory.

Introduction

Much effort has gone into the investigation of both excess electron and hole transport within DNA over the past few years; however, the transfer of electrons through DNA remains a topic of considerable interest and some controversy.[1−14] Owing to the rapid processes involved at short electron-transfer distances, the usual techniques employed have been photochemical in nature. The short time scales require spacing of donor and acceptor within a few base pairs. For this reason random distributions of intercalators cannot be used without accounting for cooperative binding effects.[15,16] To overcome the later difficulty, specific oligonucleotides with donor and acceptors at known distances have been synthesized with some success.[17−21]

An inherent difficulty in all electron-transfer studies is that the mechanism of electron transfer may not be clear. At ambient temperatures both tunneling and hopping mechanisms for electron transfer are active and not easily distinguishable unless the processes are followed explicitly.[13,22,23] For example, at this point there are a number of reports of the tunneling decay constant, β, for electron transfer within DNA that vary from 0.1 to 1.5 Å^{-1}.[2,4,6,17−19] Since hopping rates do not follow a log−distance relationship and fall off more slowly with distance than tunneling, it is becoming increasingly recognized that hopping likely accounts for low β values reported in some studies;[9,10,18,24] therefore, it is important to separate the hopping and tunneling phenomena by experimental means.

In our previous work we investigated excess electron transfer to a bromine-substituted base in DNA and found results that suggested electron hopping was the principal mode of electron migration at 200 K. A theoretical treatment that fit the data was given[23] and suggested relatively short-range electron-transfer distances at 77 K that increased very substantially when samples were annealed and hopping was activated. In most systems the relative contribution of hopping and tunneling is not known. However, the activation energy toward hopping of excess electrons has been estimated to be ca. 5 kcal/mol in one report.[25] Interestingly, this value matches the 5 kcal/mol stabilization induced by proton transfer from G to C$^{\bullet-}$ within the DNA.[14,26] The reverse process would be necessary for activation of electron transfer. The stabilization of the hole by proton transfer from G$^{\bullet+}$ to C is only slight energetically, and this suggests a lower barrier toward transfer of the hole within DNA.[14]

In this work we use a system consisting of an irradiated aqueous glass containing DNA at low temperatures. Such systems have been employed in the past to gain information on the localization of the electron and hole on DNA. For example, work with LiCl aqueous glasses containing various oligonucleotides has shown clearly that the cytosine anion is the preferred site of localization on DNA.[27−29] Further, studies with 8 M $NaClO_4$ glasses containing DNA were used to identify the localization of the hole on the guanine base in DNA.[30] This early work in glasses was later confirmed in irradiated frozen aqueous DNA solutions[31,32] where the hole was found to be

* To whom correspondence should be addressed. E-mail: Sevilla@oakland.edu. Fax: 248 370 2321.

† Present address: Department of Biochemistry and Biophysics, University of Rochester, Rochester, NY, 14642.

10.1021/jp993550w CCC: $19.00
Published on Web 01/15/2000

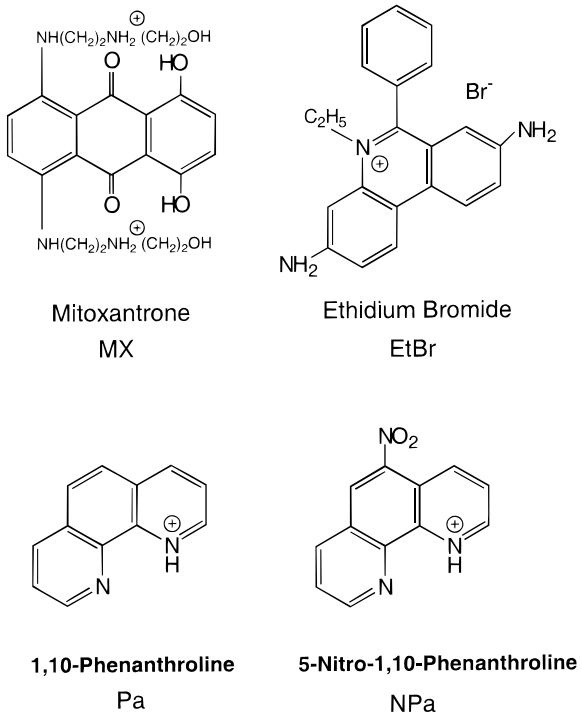

Figure 1. Structures of intercalators employed in this work.

distributed mainly on guanine and the electron mainly on cytosine with some on thymine. These radicals are found to be stable at 77 K. In these earlier studies significant activated hopping of the trapped electrons with loss of electron spin resonance (ESR) signal was not found to occur until temperatures above 160 K were reached.[31] The relatively high yields and stability of these primary ion radicals within DNA over long times are considered strong evidence that DNA is not an efficient medium for excess charge migration at low temperatures.[7]

In the present effort we employ aqueous glasses at low temperatures and ESR spectroscopy and directly observe both the DNA electron adduct and the electron adduct to selected intercalators as a function of time. At the low temperatures employed in this work the DNA electron adduct is stable and electron hopping over its activation barrier is halted; single-step tunneling becomes the only likely mode of transfer. In this work random intercalation is employed but at large spacings as low as 1 per 230 base pairs where problems in analysis introduced by cooperative effects are greatly diminished.[15] The low temperatures employed (77 K) provide for a determination of the tunneling constant β for DNA unencumbered by competing hopping mechanisms that are activated at higher temperatures.[23,31] While electron transfer by tunneling for near neighbors is fast, i.e., picoseconds,[33] as the distance increases, the time for transfer become exponentially longer, allowing for measurements to take place from minutes to days. This property of tunneling is exploited in this work. Pezeshk et al.[34] reported an earlier study of electron transfer in frozen aqueous solutions of DNA intercalated with mitroxantrone. The results found in the present work in aqueous glasses differ markedly from those of this earlier work in frozen ices that reported far greater electron-transfer distances.[34] Transfer to adjacent DNA double strands in frozen ice samples used in this earlier work is considered the likely cause of the difference. Figure 1 shows the structures of the intercalators used in this study.

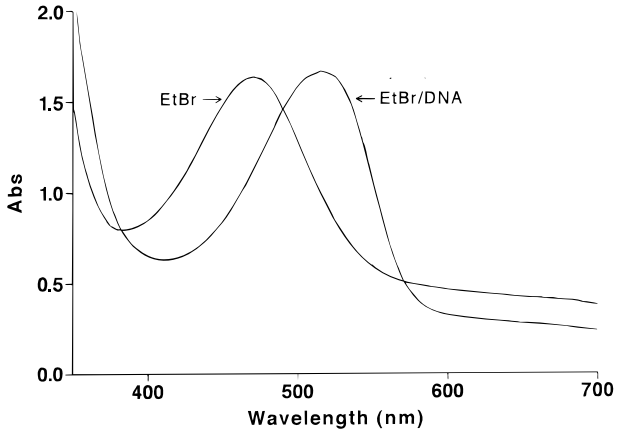

Figure 2. UV−vis spectra of ethidium bromide (0.25 mg/mL in 7 M LiBr) and of ethidium intercalated within DNA (20 mg DNA/mL, 1:50 EB/DNA BP in 7 M LiBr). The 50 nm shift in maximum intensity is in accord with intercalation within the DNA.

Experimental Section

System. Various molar ratios of salmon sperm DNA and an intercalator, mitoxanthrone (MX), ethidium bromide (EB), 1,10-phenanthroline (Pa), or 5-nitro-1,10-phenanthroline (NPa), were dissolved in a 7 M LiBr (D_2O) aqueous glass. The intercalator (I) was varied in concentration from 1 intercalator molecule per 500 base pairs (bp) to 1 per 10 bp with most work in the 1:200 to 1:20 range. The intercalators are assumed to interspace randomly within the DNA. Our results suggest that this is a reasonable assumption up to 1 intercalator per 10−20 bp. DNA was varied in concentration from 5 to 20 mg/mL without significant change in results. To ensure uniform mixing of the DNA and MX, samples were allowed to stand for long times (days to weeks) and stirred periodically all under nitrogen. Because of EB's lower binding constant uniform mixing was attained more rapidly. The fraction of intercalator unbound was small for EB and MX. For example, in Figure 2 we show the UV−vis spectra of EB (0.25 mg/mL) and Et/DNA (20 mg DNA/mL, 1:50 EB/DNA bp), respectively, in 7 M LiBr. The 50 nm shift in maximum intensity is in accord with intercalation within the DNA. In addition, the Et/DNA samples showed an increase in visible fluorescence associated with intercalation.

Typical DNA intercalator solutions were prepared by addition of 0.3 mL of D_2O to 20 mg of solid DNA/intercalator mixtures prepared beforehand by freeze-drying. After the solution was allowed to sit overnight, 0.7 mL of 10 M LiBr was added and the resulting mixture was allowed to stand for several days with occasional vortex mixing. All preparations were performed under nitrogen. The solution was drawn into a thin wall 4 mm Suprasil quartz tube and was cooled to 77 K in liquid nitrogen, producing a clear glassy solution of DNA and intercalator.

These samples were usually γ-irradiated for doses of 700 Gy (15 min). However, doses up to 2800 Gy (1 h) were not found to change results significantly. Irradiation of the 7 M LiBr glass creates electrons and holes. The electrons are scavenged by the DNA−intercalator system, and the holes remain in the glass as $Br_2^{\bullet -}$ radicals.[35] The $Br_2^{\bullet -}$ radicals have a very broad ESR spectrum that extends over many hundreds of gauss. This ESR spectrum does not interfere with the DNA and intercalator radical signals resulting from electron attachment because they extend less than 75 G. DNA makes up only 0.5%−2% of the mass of the sample. Thus, at least 98% of the initial ionizations occur in the solution. As a consequence, the DNA−intercalator system acts as the electron acceptor while the bromide ion acts

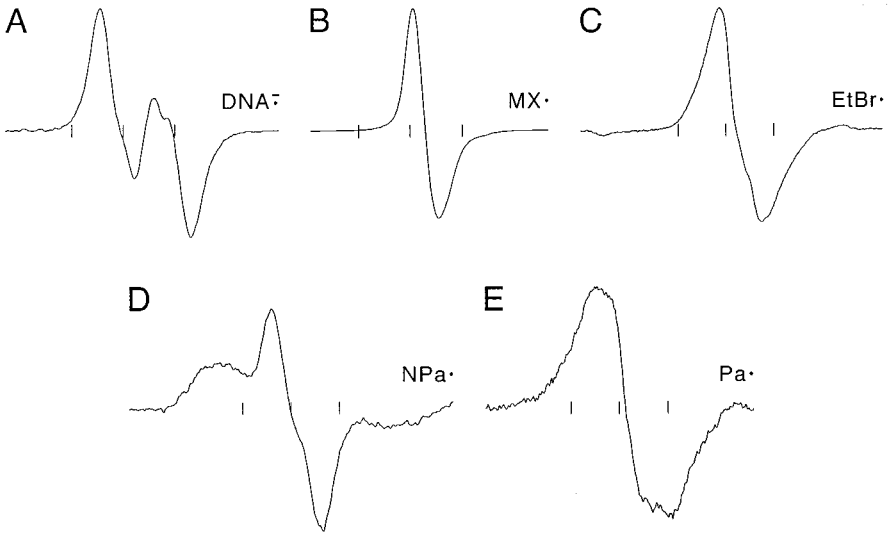

Figure 3. First derivative electron spin resonance "benchmark" spectra used in the analyses of DNA−intercalator complex systems. Each radical was produced in irradiated frozen 7 M LiBr (D_2O) glasses containing the parent compound at 77 K. For the intercalators (B−E) the spectra of the free and DNA bound intercalators did not differ significantly. (A) DNA anion (20 mg DNA/ml). (B) Mitoxantrone radical cation, $MX^{\bullet+}$. (C) Ethidium radical, $Et^{\bullet}$. (D) 5-Nitro-1,10-phenanthroline radical, $NPa^{\bullet}$. (E) 1,10-Phenanthroline radical, $Pa^{\bullet}$.

as the chief hole scavenger. This creates a DNA−intercalator ESR signal largely free from holes; as a consequence, this system is able to mediate electron transfer without significant interference from holes. ESR spectra were recorded within a few minutes after irradiation and at increasing time intervals thereafter owing to an observed log time dependence in the fraction of electrons captured by the intercalator.

Methods of Analyses. *Benchmark Spectra of DNA and Intercalator Electron Adducts*. The ESR spectra of DNA and intercalator electron adducts in 7 M LiBr were produced as benchmark spectra (Figure 3). Samples of DNA (20 mg/mL) were irradiated at 77 K for a dose of 700 Gy to produce sufficient signal of the DNA anion (Figure 3A). Samples of the intercalators were prepared in 7 M LiBr at 1 mg/mL concentration followed by γ-irradiation at 77 K. ESR spectra found for the electron adducts of the intercalators MX, EB, NPa, and Pa are shown in parts B, C, D, and E of Figure 3, respectively. Spectra found by subtraction of the DNA signal from a combined spectrum of intercalator and DNA gave spectra indistinguishable from benchmark spectra shown in Figure 3. An advantage to our analyses is that the doublet DNA ESR spectrum and the single-line ESR spectra of the one-electron reduced intercalators, MX and EB, are nearly orthogonal. This creates an excellent system for analyses of the relative fraction of each in a spectrum, that is, a combination of DNA and intercalator electron adducts. Linear least-squares fitting of benchmark to experimental spectra[23] was employed to determine the fractional composition of intercalator and DNA electron adducts. The dotted lines in Figure 4 show the fits to experiment. The spectra of Pa and NPa electron adducts are broader than those of the MX or EB electron adducts, but reasonable results (not shown) were also found in this system. NPa and Pa require lowering of the pH slightly (pH 5) to maintain their protonated states. We found that the unprotonated NPa and Pa were relatively unreactive to the electron compared to the protonated species.

The ESR signals of the intercalator and DNA electron adducts were time-dependent, with the intercalator electron adduct increasing with time and the DNA electron adduct decreasing with time. Within experimental error, at higher loadings of intercalator the overall ESR signal intensity was constant over the time frame of the experiments. Some loss of total signal was apparent at long times with loadings below 1/100 bp. This was attributed to the electron transfer from the DNA radical to the matrix hole. At higher loadings, electron transfer to the hole was not competitive with transfer to the intercalator.

Photobleaching experiments with light from an incandescent lamp showed that the DNA electron adduct photodetached with concomitant electron transfer to MX and hole. The MX electron adduct was not affected by visible light. However, for EtBr/DNA samples it was found that photobleaching removed both the DNA and intercalator electron adducts, resulting in return of the electron to the hole. This indicates that MX is a deep trap, whereas EtBr only weakly binds the electron.

Results

Mitoxantrone. In Figure 4A we show ESR spectra initially found after 15 min of γ-irradiation of samples containing 20 mg/mL DNA in 7 M LiBr at various loadings of mitoxantrone. As the loading of the intercalator increases, the MX electron adduct radical increases relative to the DNA anion radical. Least-squares fits (shown in Figure 4A) at the lowest loading of MX (228 bp/1 MX) give 8.7% of the electrons on MX and 91.3% on DNA, whereas at the highest loading (23 bp/1 MX) 59% are captured by MX and 41% of electrons remain on DNA.

The total radical intensities of the DNA samples at various loadings of intercalator were found to be the same; i.e., DNA samples at low and high loadings gave the same number of total spins (DNA + MX radicals) within experimental error. This is good evidence that MX does not increase the scavenging efficiency of the DNA, which is a basic assumption in our work.

Samples were held at 77 K during and after irradiation, and electron transfer from DNA to MX was periodically monitored over time by analyses of the ESR spectra. In Figure 5 we show the time dependence of the fraction of MX radical for the various loadings investigated. The fraction of total electrons captured by MX (F_{MX}) is found to be approximately linear with the natural log of time as expected for a tunneling process between reagents randomly dispersed in a rigid matrix.[36] Least-squares fits to a linear log time relation are shown in Figure 5. We note, however, that over large changes in F, only plots of $\ln(1 - F_{MX})$ vs $\ln(t)$ will be linear (see theoretical development presented below).

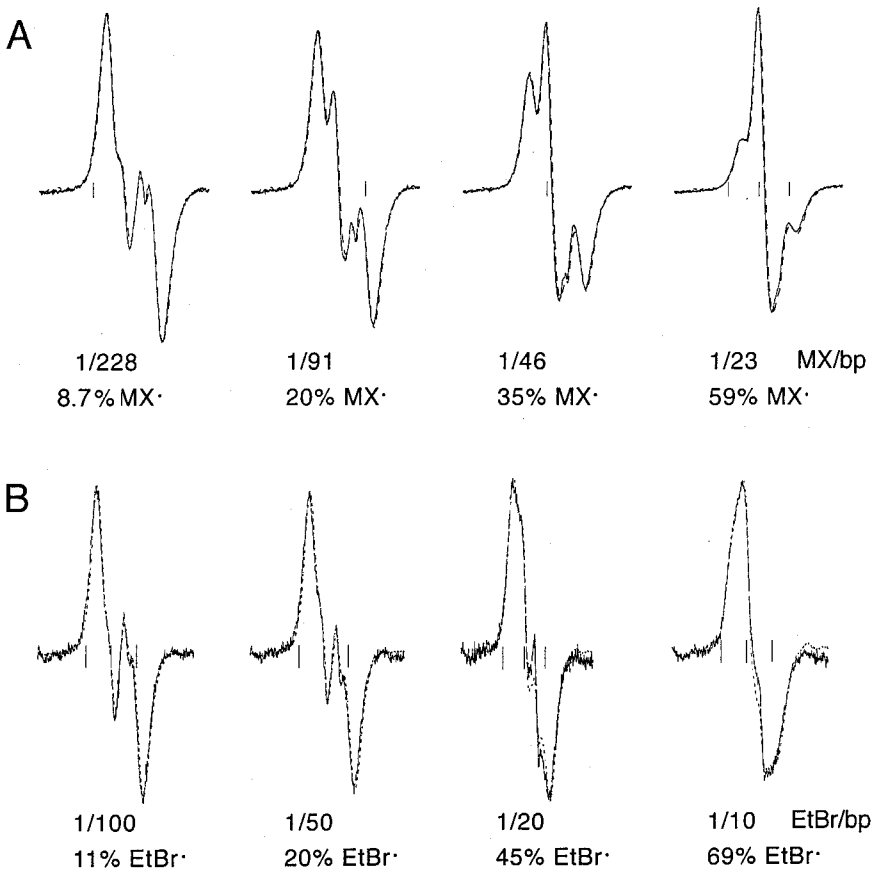

Figure 4. First derivative electron spin resonance spectra show spectra found immediately after γ-irradiation of samples of 20 mg/mL DNA in 7MliBr with various loadings of mitoxantrone (A) and ethidium bromide (B). The dashed spectra are simulations made by linear least-squares fits of the benchmark functions (Figure 3A,B for MX or Figure 3A,C for EtBr) to experimental spectra. The spectra clearly show that the intercalator radical increases in relative amount to the DNA anion radical with increased loading of intercalator. At the lowest loading of MX (228 bp/1 MX) these fits suggest that 8.7% of the electrons are found on MX, whereas at the highest loading (23 bp/1 MX) 59% are captured by MX with the remainder on DNA. For EtBr the fraction of electrons captured at the same loading is about half of that found for MX. The fraction of electrons captured by each intercalator increases with time.

To investigate the possibility of electron transfer from one DNA double strand to another, a dilution study was performed. Three differing DNA concentrations (circles, 20 mg/ml DNA; squares, 10 mg/mL DNA; triangles, 5 mg/mL) were employed all at 46 bp/1 MX. As can be seen in Figure 5, no significant differences are found with 4-fold dilution. If transfer between individual DNA double strands were occurring, the MX radical fraction would decrease with dilution. Since this does not occur, we conclude that no substantial transfer between the double-stranded helixes occurs in these glassy matrices. The average separation between strands at 20 mg DNA/mL is about 140 Å and at 5 mg DNA/mL is 280 Å. Since our analyses (see below) suggest transfer distances to be no more than 35 Å, the lack of transfer between double strands at these concentrations is quite reasonable.

Ethidium Bromide. In Figure 4B we show ESR spectra found after γ-irradiation of samples of 20 mg/mL DNA in 7 M LiBr with various loadings of ethidium bromide. Samples were again held at 77 K during and after irradiation, and electron transfer from DNA to EtBr was monitored over time by analyses of the ESR spectra. The simulations based on the benchmark spectra in Figure 3 are overlaid over the experimental spectra. Figure 6 shows a plot of the fraction of total electrons captured by EtBr versus the natural log of time found for the various EtBr/DNA (bp) ratios. Ethidium is clearly a poorer electron scavenger than MX. Capture of 50% of the electrons by EtBr occurs at higher loadings (about a factor of 2) than for MX, suggesting a shorter scavenging range by about half for EtBr.

1,10-Phenanthroline (Pa) and 5-Nitro-1,10-phenanthroline (NPa). Experiments identical to those performed for MX and EtBr were performed with 1,10-phenanthroline (Pa) and 5-nitro-1,10-phenanthroline (NPa) as intercalators. The electron-scavenging abilities of these intercalators are between those or EtBr and MX, and not unexpectedly, the addition of the nitro group substantially increases the scavenging range of the phenanthroline moiety. Analyses of these results are presented below.

Analysis for Distances, Rates, and Tunneling Constant. Figure 7 depicts a section of DNA with random intercalations. D is the time-dependent scavenging range and can be considered the average tunneling distance in base pairs from the electron adduct on DNA to the intercalator at the time of measurement. For random intercalation, the probability that at least one scavenger is present within D base pairs (the capture distance) from the trapped electron is given by

$$F(t) = 1 - (1 - \nu)^{2D(t)} \quad (1)$$

where ν is the intercalator (I) to base pair (bp) mole ratio, ν = I/bp. $F(t)$ represents the fraction of all electrons added to DNA that are captured by the intercalator in time t. Figure 8 shows a plot of F vs ν for MX and EtBr at 1 min. The lines are fits of eq 1 to the data for $D = 9.5$ bp for MX and $D = 4.2$ bp for EtBr. As can be seen, eq 1 accounts for the dependence of electron capture with intercalator loading. The only obvious

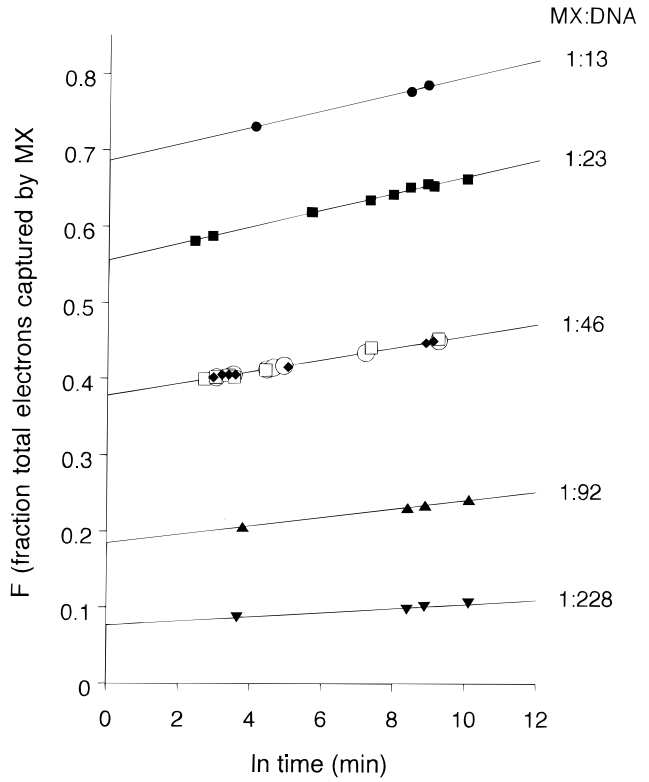

Figure 5. Plot of the fraction of total electrons captured by MX (F) vs the natural log of time found for various MX/DNA (bp) ratios. Samples were held at 77 K during and after irradiation, and electron transfer from DNA to MX was periodically monitored over time by analyses of the ESR spectra. For the 46−1 loading, three differing DNA concentrations (circles, 20 mg/mL DNA; squares, 10 mg/mL DNA; triangles, 5 mg/mL) were employed. No significant differences are found with dilution, suggesting that little or no transfer from one double-stranded helix to another is occurring.

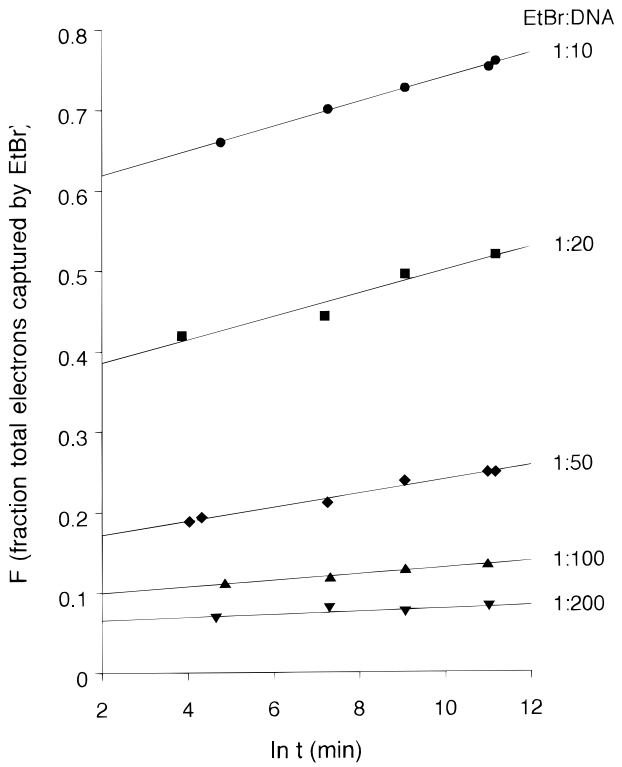

Figure 6. Plot of the fraction of total electrons captured by ethidium (F) vs the natural log of time found for the various Et/DNA (bp) ratios. Samples were held at 77 K during and after irradiation, and electron transfer from DNA to Et was monitored over time by analyses of the ESR spectra as shown in Figure 3.

deviation is for MX at high loading. Reasons for this are discussed below.

The relation for the time-dependent scavenging distance, $D(t)$, is obtained by a simple rearrangement of eq 1 and is given by

$$D(t) = \frac{\ln(1 - F(t))}{2\ln(1 - \nu)} \tag{2}$$

Since ν is almost always small compared to 1, this becomes

$$D(t) = \frac{-\ln(1 - F(t))}{2\nu} \tag{3}$$

In the limit as the intercalator loading (ν) approaches zero, F also becomes small with 1 and the relation becomes $D \approx F/(2\nu)$. The limiting slope in the plot of F vs ν is $2D$ (Figure 8) as reported in our earlier work.[23] In this work we find that the distances calculated by eq 2 are constant over wide ranges of intercalator loadings at any time t and are equal to those found from the extrapolation to zero intercalator loading.

For the time dependence of D we employ the approximation, successfully used for tunneling kinetics in glasses,[36] that all electrons that have a scavenger closer than D tunnel to the scavenger by the time of observation t while all other electrons remain trapped (the exact condition for D is $k_o\, e^{-\beta D}t = 1$). This results in the following relation:[36]

$$D(t) = (1/\beta)\ln(k_o t) \tag{4}$$

where k_o is the fundamental electron-transfer rate (constant) and

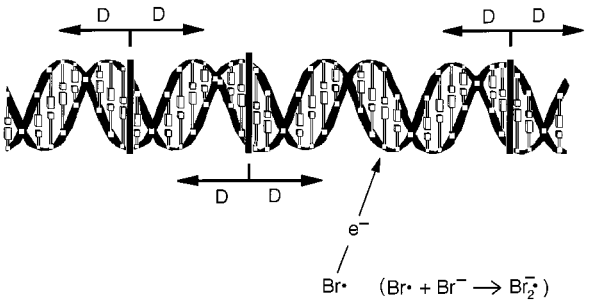

Figure 7. Diagram depicting random intercalator spacings and the scavenging range of the intercalator (D). D is time-dependent and extends outward in time. It can also be considered the electron-transfer distance to the intercalator. At high intercalator loadings the scavenging ranges have a higher probability for overlap as shown on the left side of the diagram. We find that this is well accounted for by eq 1. The electron that adds to DNA is produced by radiation of the matrix (7 M LiBr, D_2O), which leaves a hole in the matrix as $^{\bullet}Br_2^-$.

D and β are in bp and bp^{-1}, respectively. Plots of D vs $\ln(t)$ are expected to be linear with the slope equal to $1/\beta$ and intercept of $(1/\beta)\ln k_o$. Such plots are shown in Figure 9 for MX and EtBr. All values of ν except $^1/_{13}$ for MX and $^1/_{200}$ for EtBr are shown. All values of $D(1')$, β, and k_o calculated from such plots are given in Table 1 for MX, Table 2 for EtBr, and Table 3 for NPa and Pa.

The transfer distances reported in Tables 1 and 2 show the quality of the fit of our data for MX and EtBr to eq 2. The data in Table 1 for MX and Table 2 for EtBr show similar values for distance regardless of loading and suggest that the assumption of random intercalation appears to hold to DNA(bp)/MX ratios of 20 or more and for DNA/EtBr for 10 or more. Deviations from eq 2 are expected at very high loadings of intercalator where nonrandom intercalation may occur. Indeed

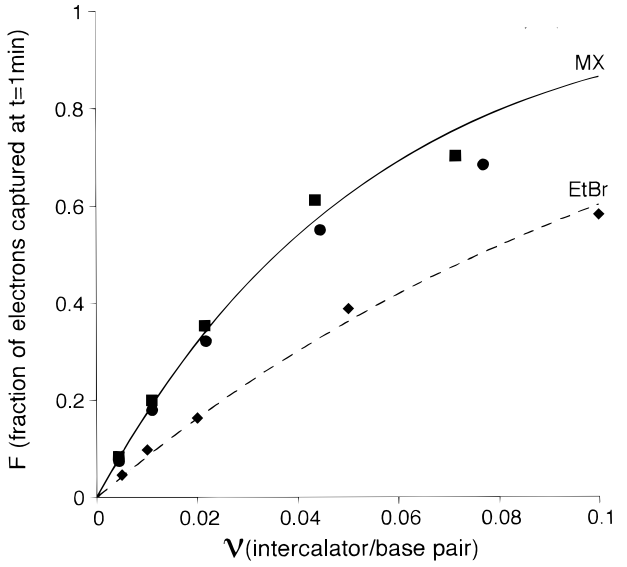

Figure 8. Plot of the fraction of total electrons captured by MX and Et at 1 min vs the intercalator loading. The curves are fits to the function $F = 1 - (1 - \nu)^{2D}$. The curvature is a result of the overlap of scavenging ranges of the intercalators when the range, D, is no longer small with respect to $1/\nu$. The two sets of points for MX are found for two separate experiments done after 1 h irradiation (circles) and 15 min irradiation (squares). The line is a fit to the overall data and gives D of 9.5 for MX and 4.2 for EtBr. Deviations from the function are expected at high loadings of intercalator where cooperative effects may occur.

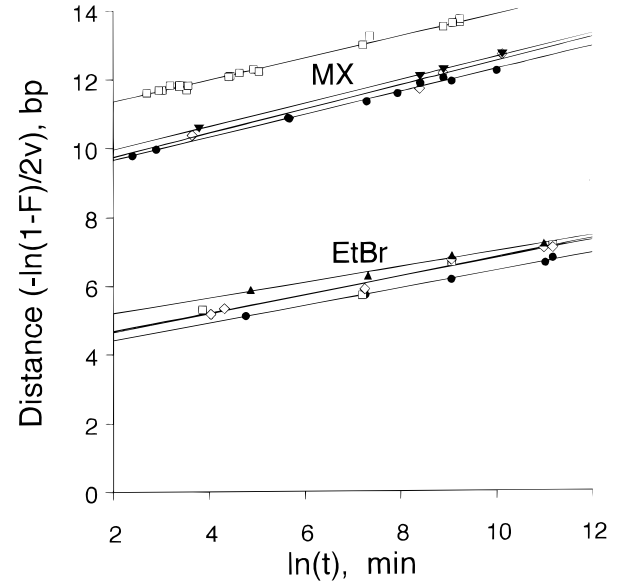

Figure 9. Plot of electron-transfer distance in base pairs computed from $-\ln(1 - F)/(2\nu)$ vs natural log of time in minutes for DNA samples at various intercalator loadings. The upper traces show results for the intercalator, mitoxantrone (MX), at the following DNA(bp)/MX mole ratios: filled circles, 23/1; squares, 46/1; filled triangles, 92/1; diamonds, 228/1. The lower traces show results for ethidium bromide (EtBr) at the following DNA(bp)/EtBr mole ratios: filled circles, 10/1; squares, 20/1; diamonds, 50/1; filled triangles, 100/1. The slope of each line is $1/\beta$, and the intercept is $(1/\beta)\ln(k_o)$.

the highest DNAbp/MX ratio of 13 does show a smaller transfer distance than the remainder of the loadings. This may be the result of some cooperative intercalation. The fact that the distances calculated were relatively uniform with ratios of 230/1 to 23/1 suggests no substantial cooperative effects in this range. Deviations from the relation of distance and time (eq 4) are expected at very low loadings where the competition from the holes in the matrix may be encountered. For EtBr the lowest loading of $^{200}/_{1}$ shows a higher distance (greater scavenging than the others). This might be expected for competition from holes in the matrix, but the reduced signal levels also create greater uncertainty in this case. However, as can be seen in Figure 9, the remainder of the loadings give similar values for slopes and intercepts.

TABLE 1: Results for Electron Scavenging Distance, β, and Rate vs Intercalator Loading for Mitoxantrone[a]

$1/\nu$ bp/MX	$D(1')$ (bp)	n	β (Å^{-1})	$\log_{10}(k_0)$ (k_0: s^{-1})
13	7.1 ± 0.2	3	1.0 ± 0.2	9 ± 2
23[c]	9.0 ± 0.1	10	0.90 ± 0.04	10.2 ± 0.6
23[c]	9.4 ± 0.1	3	1.0 ± 0.1	11.6 ± 0.3
46[b,c]	10.7 ± 0.1	21	0.92 ± 0.04	12.7 ± 0.8
46	8.9 ± 0.4	4	0.94 ± 0.12	11 ± 2
92	9.3 ± 0.1	3	0.9 ± 0.1	10.3 ± 1
228	9.1 ± 0.1	4	0.9 ± 0.2	10 ± 2

[a] $D(1')$ is the calculated distance or scavenging range at 1 min. β is the tunneling distance decay constant. Both result from a fit of D vs $\ln(t)$ (eq 8). $1/\nu$ is the number of base pairs per intercalator. [b] These data are a compilation of three runs at 5, 10, and 20 mg DNA/mL. No statistical difference in results was found in the individual runs, and the overall fit is reported here. [c] γ-Irradiations were 60 min except for these results, which were 15 min. No significant difference was noted in the results.

TABLE 2: Results for Distance, β, and Rate vs Intercalator Loading for EtBr

$1/\nu$	$D(1')$ (bp)	n	β (Å$^{-1)}$)	$\log_{10}(k_0)$ (k_0: s^{-1})
10	3.9 ± 0.2	5	1.18 ± 0.08	4.5 ± 0.6
20	4.2 ± 0.8	4	1.2 ± 0.4	5 ± 3
50	4.1 ± 0.4	6	1.1 ± 0.2	4.5 ± 1.2
100	4.8 ± 0.4	4	1.34 ± 0.26	
200	6.3 ± 1.8	4		

TABLE 3: Results for Distance, β, and Rate vs Intercalator Loading for NPa and Pa

I	$1/\nu$	$D(1')$ (bp)	n	β (Å^{-1})	$\log_{10}(k_0)$ (k_0: s^{-1})
NPa	20	9.4 ± 0.4	5	1.0 ± 0.2	12 ± 4
NPa	39	8.2 ± 0.6	10	0.8 ± 0.2	8 ± 3
NPa	49	8.1 ± 1.0	10	0.8 ± 0.2	8 ± 4
NPa	100	7.4 ± 1.8	10	0.9 ± 0.6	9 ± 5
Pa	24	5.5 ± 1.2	5	1.8 ± 1.6	*a*
Pa	69	4.9 ± 1.4	5	*a*	*a*

[a] These values were not statistically significant at 2σ.

We note that in general the rate of electron transfer is given by $k_{et} = (1/\beta)\,dD/dt$. Therefore, values of dD/dt at any time t and distance D can be used as a direct measure of the electron-transfer rate, k_{et}. We also note that calculations using the more conventional tunneling relation, $k_{et} = k_0\, e^{-\beta D}$, the relation between dD/dt and k_{et}, and the fact that $dD/dt = 2\nu F'(t)/(1 - F(t))$ result in the same values for β and k_0 as found from eq 4.

Values of β. As shown in Table 4, we find that the values of β are near 1 with slightly lower values for NPa and MX (ca. 0.8−0.9 Å^{-1}) and a slightly higher value for EtBr of 1.2 Å^{-1}. The value of β does not appear to be the major reason for the difference in transfer distances, although it does contribute. Differing fundamental rates appear to be the major effect.

Rates of Electron Transfer. The rates of electron transfer we measure are quite small. Even for MX, which has the highest rate, it is only about 0.005 s^{-1} at 1 min after irradiation where D is about 10 bp. Yet for MX we find that k_o is $10^{11\pm2}$ s^{-1} (with slower rates for other intercalators, Tables 1−3). The

TABLE 4: Summary of Best Estimates of Electron Transfer Distances, Tunneling Constants, and Calculated Electron Affinities[a]

intercalator	D (t = 1 min) (bp)	β (Å^{-1})	log k_o (k_o: s^{-1})	calcd EA (eV)
MX	9.5 ± 1.0	0.92 ± 0.1	11 ± 2	-6.25
NPa	8.3 ± 1.0	0.85 ± 0.2	9 ± 3	-5.89
Pa	5.2 ± 1.0			-5.21
EtBr	4.2 ± 0.5	1.2 ± 0.2	5 ± 1	-4.32

[a] Theoretically calculated electron affinities were computed with the DFT method at the pBP86/DN*//DN level by subtraction of the total energy of the parent molecule from that of the electron adduct in the geometry of the parent molecule.

expected maximum values[37] for the fundamental value of k_o are on the order of 10^{13} s^{-1}, and values near this have been reported,[8,16,20] but lower values are typical for excess electron transfer.[25] Clearly, our work with various intercalators suggests that the rate is dominated by the nature of the intercalator (e.g., electron affinity and strength of binding within DNA). This result has been found in other work[9,16,23,25] and is expected from theory.[4,8,38] The fact that our value of k_o for MX, measured at 77 K, is close to values measured at elevated temperatures suggests only a small thermal contribution to the tunneling rate constant for this intercalator. We plan to test this with further studies at liquid helium temperatures.

Calculation of Intercalator Electron Affinities and Their Relation to *D* and *β*. The nature of the intercalator clearly is correlated with the electron-transfer distance we measure. One important property related to electron-transfer rates is the free energy change for the transfer.[8] The redox potentials for the intercalators in the same solvent system are not available for the intercalators used in this study, so we have calculated the electron affinities of the intercalators. The electron affinity is a dominant term in the relative free energy change for electron transfer from the DNA electron adduct site to the intercalator. Calculation of the electron affinities was performed using density functional theory at the pBP86 level with the DN* basis set. The method was employed to optimize the structures with the DN basis set and to perform single-point calculations with the DN* basis set for the parent and electron adduct. The electron affinity was determined from the difference between the total energy of the parent and that of the electron adduct. Since reorganization of the electron adduct was not allowed, the values reported in Table 4 are those for the vertical electron affinities. All intercalators were positively charged, and thus, electron reduction has a strong Coulombic term. This term would be substantially diminished in a polar solvent, and thus, the values are likely overestimates of the electron affinities. The relative values, however, should be appropriate to compare to the distances for electron migration found in this work. In Figure 10 we show the distances of electron transfer vs the calculated electron affinities. A good correlation exists between electron affinity and distance, which suggests that the transfer rates increase as the free energy for electron transfer becomes more negative, suggesting that the system is not in the Marcus inverted region.[6,37] Values of β for the intercalators reported in Table 4 have slightly lower values for the intercalators with larger electron affinities, MX and NPA, and a slightly higher value for EtBr, which has lower electron affinity, EtBr. The combined effect of the lower free energy for transfer and the higher value of β makes EtBr a poor scavenger for excess electrons.

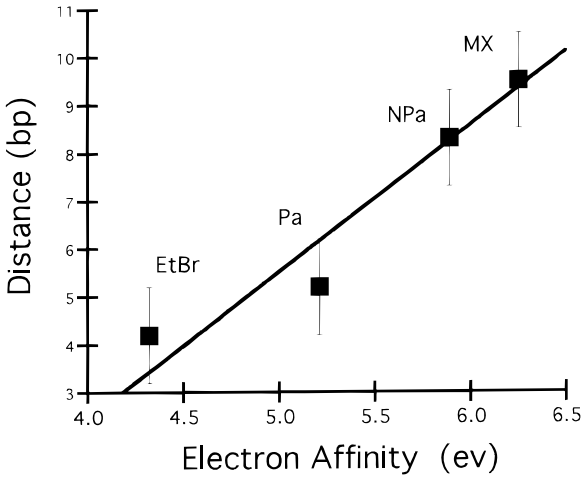

Figure 10. Experimentally determined scavenging distance at 1 min for various intercalators vs their calculated electron affinities. The density functional theory calculations were performed at the pBP86/DN*//DN level. A good correlation exists between electron affinity and distance, which suggests that the transfer rates increase with increasing intercalator electron affinity (or more negative free energy for electron transfer).

Discussion

Our major findings are the following.

1. Electron-transfer distances computed from eq 1 are found to be independent of intercalator loading over a large range of loadings. Equation 1 assumes a random insertion of intercalators and apparently adequately describes the distribution of intercalators within DNA from low to moderate loadings. Only at high loadings are deviations found. The fact that native DNA was used means that these results should be considered averages over many different base sequences.

2. The electron-transfer rates are time-dependent and vary with log time from minutes to weeks in accord with a one-step tunneling process. Other ESR studies have shown that electron migration by hopping is not significant until temperatures near 200 K are reached,[23] and the activation energy for hopping of the excess electron is estimated to be 5 kcal/mol.[25] Thus, no activated hopping is likely at 77 K and tunneling is the likely mechanism.

3. Results show that electron-transfer distances at 1 min range from 4 to 10 base pairs. These distances are not especially large (<35 Å) and do not suggest unusual rates or mechanisms of excess electron transfer through DNA. The relatively small transfer distances for EtBr and Pa suggest a slow fundamental rate for the transfer at 77 K.

4. The β values found are from 0.8 to 1.2 Å^{-1} and are in the "usual" range for DNA and protein systems.[4,6] However, in this work the low temperatures (77 K) employed make it more likely that the DNA base pairs are well stacked and do not undergo significant librational motions. This should create an improved coupling through the DNA stacked π-systems. In addition, the electron in these systems resides in the LUMO of the DNA bases cytosine and thymine.

5. We find that the transfer distances and fundamental rates do correlate with the intercalator electron affinity as suggested in earlier reports.[9,25] A higher intercalator electron affinity results in a greater driving force for electron transfer that increases the electron-transfer rate (when not in the Marcus inverted region).

Several studies do report lower values for β than found in this work, but these are usually for electron transfer through hole transfer (HOMO) and not excess electron transfer (LUMO). For example, Meggers et al.[18] find a β of 0.7 Å^{-1} for hole transfer from G+ to GGG but found that intermediate AT base pairs greatly slowed the transfer and that a hopping mechanism

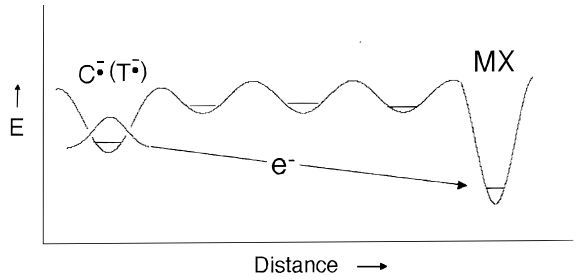

Figure 11. Diagram depicting single-step electron transfer from a trapping site at the DNA base cytosine (or thymine) to an intercalator. The electron trapped on cytosine or thymine is energy-stabilized by nuclear reorganization after electron attachment. The cytosine anion radical is further stabilized by proton transfer from guanine. Transfer to other bases, depicted as shallow wells, is believed to be thermally inaccessible at 77 K. Thus, hopping is eliminated and a single-step tunneling occurs.

to intermediate G in the sequence likely explains the strong sequence dependence found. Lewis et al.[20] report a value of 0.64 for hole transfer to G through AT sequences, which appears to be in apparent disagreement; however, the coupling of the stilbene acceptor to DNA was covalent and this may allow for stronger modes of transfer. Several authors suggest[1,22] that the earlier reports[9] of very low β values from 0.1 to 0.5 $Å^{-1}$ are likely a result of multiple hopping steps and not single-step tunneling. Hopping rates are likely more limited for excess electron transfer vs those reported for hole transfer because of the extra stabilization provided by proton transfer to the electron adduct in the GC base pair.[14,26] In DNA the GC base pair is the locus for hole stabilization (on G), but proton transfer does not provide substantial stablilization. The major locus for electron stabilization is also in the GC base pair (on C). The electron localizes on thymine to a lesser extent, and it is not clear at present if transfer from C, T, or both is observed in our system.

Another mechanism recently proposed is a phonon-assisted hopping mechanism.[24] This mechanism cannot be operative in our case owing to the low temperatures and frozen systems used in this work that prevent any large-scale motional activity. However, tunneling between equivalent C or T sites in DNA might seem to be possible, and this would allow for long-range transfer. However, we have no evidence for such a "tunneling−hopping" mechanism. A likely reason for this is that tunneling does not occur uphill and that the stabilization provided by nuclear reorganization and possible proton transfer on electron addition to cytosine or thymine amounts to a significant energy difference between donor (e.g., $C^{\bullet -}$) and acceptor (e.g., C). This energy difference is apparently not accessible by tunneling or thermal activation at 77 K. Thus, the tunneling we observe is downhill and proceeds through a one-step tunneling mechanism between the original electron addition site and the intercalator. A diagram depicting single-step electron transfer from a trapping site at the DNA base cytosine to an intercalator, illustrating this point, is shown in Figure 11.

Reports in which radiation produced hydrated electrons add to DNA in aqueous solutions at ambient temperatures suggest that electron migration occurs from a few bases pairs[25,39] to about eight base pairs.[40] No time scale is reported, so these can be viewed as the relative rates of electron transfer to other processes such as irreversible protonation reactions.[31] In contrast to these somewhat short distances for radiation-produced excess electrons, a recent study reports results for hole transfer at ambient temperatures that extend beyond 30 base pairs.[41] These results are in keeping with photochemical results for hole transfer[1,9−11,18] in which long-range transfer is found and are likely explained by the lack of an irreversible proton-transfer process for the guanine cation radical that allows time for multiple thermally activated hopping steps.

Pezeshk et al.[34] reported a study similar to this for frozen aqueous solutions of DNA intercalated with MX. These solutions do not glass on freezing but form heterogeneous systems of ice and hydrated DNA with MX. Pezeshk et al. found numbers for excess electron transfer of 30 bp or more at 77 K, in contrast to our value of 10 bp in glassy solutions. We have repeated these experiments in similar frozen ices and found values similar to those reported by Pezeshk et al., i.e., apparent electron-transfer distances of over 30 base pairs. In addition, a number of other radiation studies of electron transfer in other solid DNA samples have also reported long-range transfer of the electron.[42] Our work suggests at low temperatures excess electron-transfer distances should be limited by a single-step tunneling mechanism. Distances of 30 base pairs (100 Å) are not realistic for this mechanism. There are several possible explanations for this apparent contradiction between results found in solution and in more concentrated frozen solid systems. We believe one explanation is electron transfer to adjacent double strands, and this mechanism is now currently under active study in our laboratory.

Acknowledgment. This research was supported by NIH NCI Grant RO1 CA45424 and by Oakland University Research Excellence Fund. K.C. is a Howard Hughes Undergraduate Scholar. D. Becker is thanked for helpful discussions.

References and Notes

(1) Ratner, M. *Nature* **1999**, *397*, 480.
(2) Turro, N. J.; Barton, J. K. *J. Biol. Inorg. Chem.* **1964**, *3*, 201.
(3) Diederichsen, U. *Angew. Chem., Int. Ed. Engl.* **1997**, *36*, 2317.
(4) Beratan, D.; Priyadarshy, S.; Risser, S. M. *Chem. Biol.* **1997**, *4*, 3.
(5) Risser, S. M.; Beratan, D. N.; Meade, T. J. *J. Am. Chem. Soc.* **1993**, *115*, 2508.
(6) Netzel, T. L. *J. Biol. Inorg. Chem.* **1998**, *3*, 210.
(7) Debije, M. G.; Milano, M. T.; Bernhard, W. A. *Angew. Chem., Int. Ed. Engl.* **1999**, *38*, 2752.
(8) Harriman, A. *Angew. Chem., Int. Ed. Engl.* **1999**, *38*, 945.
(9) Holmlin, R. E.; Tong, R. T.; Barton, J. K. *J. Am. Chem. Soc.* **1998**, *120*, 9724.
(10) Kelley, S. O.; Barton, J. K. *Science* **1999**, *283*, 375.
(11) Nunez, M.; Hall, D. B.; Barton, J. K. *Chem. Biol.* **1999**, *6*, 85.
(12) Kelley, S. O.; Barton, J. K. *Met. Ions Biol. Syst.* **1998**, *36*, 211.
(13) Sevilla, M. D.; Becker, D.; Razskazovskii, Y. *Nucleonika* **1997**, *42*, 283.
(14) Steenken, S. *Biol. Chem.* **1997**, *378*, 1293.
(15) Olson, E. J. C.; Hu, D.; Hoermann, A.; Barbara, P. F. *J. Phys. Chem. B* **1997**, *101*, 299.
(16) Brun, A.; Harriman, A. *J. Am. Chem. Soc.* **1992**, *114*, 3656.
(17) Fukui, K.; Tanaka, K.; Fujitsuka, M.; Watanabe, A.; Ito, O. *J. Photochem. Photobiol. B.* **1999**, *50*, 18.
(18) Meggers, E.; Michel-Beyerle, M. E.; Giese, B. *J. Am. Chem. Soc.* **1998**, *120*, 12950.
(19) Lewis, F. D.; Letsinger, R. L. *J. Biol. Inorg. Chem.* **1998**, *3*, 215.
(20) Lewis, F. D.; Wu, T.; Zhang, Y.; Letsinger, R. L.; Greenfield, S. R.; Wasielewski, M. R. *Science* **1997**, *277*, 673.
(21) Dandliker, P. J.; Holmlin, R. E.; Barton, J. K. *Science* **1997**, *275*, 1465.
(22) Jortner, J.; Bixon, M.; Langenbacher, T.; Michel-Beyerle, M. E. *PNAS* **1998**, *95*, 12759.
(23) Razskazovskii, Y.; Swarts, S. G.; Falcone, J. M.; Taylor, C.; Sevilla, M. D. *J. Phys. Chem. B* **1997**, *101*, 1460.
(24) Henderson, P. T.; Jones, D.; Hampikian, G.; Kan, Y.; Shuster, G. B. *Proc. Natl. Acad. Sci. U.S.A.* **1999**, *96*, 8553.
(25) Anderson, R. F.; Patel, K. B.; Wilson, W. R. *J. Chem. Soc., Faraday Trans.* **1991**, *87*, 3739.
(26) Colson, A. O.; Besler, B.; Sevilla, M. D. *J. Phys. Chem.* **1992**, *96*, 9788.
(27) Bernhard, W. A. In *The Early Effects of Radiation on DNA*; Fielden, E. M., O'Neill, P., Eds.; Springer-Verlag: Berlin, Heidelberg, 1991; pp 141−154.
(28) Bernhard, W. A. *J. Phys. Chem.* **1989**, *93*, 2187.

(29) Cullis, P. M.; Evans, P.; Malone, M. E. *Chem. Commun.* **1996**, 985.
(30) Sevilla, M. D.; D'Arcy, J. B.; Morehouse, K. M.; Engelhardt, M. L. *Photochem. Photobiol.* **1979**, *29*, 37.
(31) Yan, M.; Becker, D.; Summerfield, S.; Renke, P.; Sevilla, M. D. *J. Phys. Chem.* **1992**, *96*, 1983.
(32) Wang, W.; Yan, M.; Becker, D.; Sevilla, M. D. *Radiat. Res.* **1994**, *137*, 2.
(33) Wan, C.; Fiebig, T.; Kelley, S.; Treadway, C. R.; Barton, J. K.; Zewail, A. H. *Proc. Natl. Acad. Sci. U.S.A.* **1999**, *96*, 6014.
(34) Pezeshk, A.; Symons, M. C. R.; McClymont, J. D. *J. Phys. Chem.* **1996**, *100*, 18562.
(35) Champagne, M. H.; Mullins, M. W.; Colson, A. O.; Sevilla, M. D. *J. Phys. Chem.* **1991**, *95*, 6487.
(36) Zamaraev, K. I.; Khairutdinov, R. F. *Russ. Chem. Rev.* **1978**, *47*, 518.
(37) Netzel, T. L. In *Molecular and Supramolecular Photochemistry Series 2*; Ramamurthy, V., Schanze, K. S., Eds.; Marcel Dekker: New York, 1998; pp 1−54.
(38) Priyadarshy, S.; Risser, S. M.; Beratan, D. N. *J. Biol. Inorg. Chem.* **1998**, *3*, 196.
(39) Whillans, D. W. *Biochim. Biophys. Acta* **1975**, *414*, 193.
(40) Fuciarelli, A. F.; Sisk, E. C.; Zimbrick, J. D. *Int. J. Radiat. Biol.* **1994**, *66*, 505.
(41) Martin, R. F.; Anderson, R. F. *Int. J. Radiat. Oncol., Biol., Phys.* **1998**, *42*, 827.
(42) O'Neill, P.; Fielden, M. In *Advances in Radiation Biology*; Lett, J. T., Sinclair, W. K., Eds.; Academic Press: San Diego, CA, 1993.